Electronic Supplementary Material (ESI) for Materials Chemistry Frontiers.


# Supporting Information

## Reticular control of interpenetration in a heterogeneity metal-organic framework

Trang T. M. Nguyen,[a] Hung M. Le,[a] Yoshiyuki Kawazoe,[b] and Ha L. Nguyen*[a],[c]

[a]Center for Innovative Materials and Architectures (INOMAR), Vietnam National University–Ho Chi Minh City (VNU–HCM) 721337 Vietnam

E-mail: nlha@inomar.edu.vn

[b]New Industry Creation Hatchery Center, Tohoku University, Sendai, 980-8579, Japan

[c]Center for Research Excellence in Nanotechnology (CENT), King Fahd University of Petroleum and Minerals, Dhahran 31261, Saudi Arabia

## Table of Contents

## Section 1: Materials and General Methods

**Chemicals used in this work.** 1,3,5-triphenylbenzene (97% purity), 3-nitrobenzoic acid (99 % purity), and sodium thiosulfate pentahydrate (99.9 % purity) were obtained from Aldrich Chemical Co. D-glucose (97% purity), acetyl chloride (99.5 % purity) and ethanol (99.5 % purity) were purchased from Merck Millipore Co. Sodium hydroxide (97% purity) and sodium sulfate (97% purity) were purchased from Fisher Scientific. Biphenyl-4,4′-dicarboxylic acid (99% purity) were purchased from TCI America. Aluminum chloride (anhydrous), iron (III) nitrate nonahydrate (98% purity), dichloromethane (99.8% extra dry grade), *N,N*-dimethylformamide (DMF; 99.8% extra dry grade), acetic acid (99.5% purity), acetone (99.8% extra dry grade), and 1,4-dioxane (99.9% extra dry grade) were purchased from Acros Organics. NMR solvents: $D_2O$, $NaOD/D_2O$ 40 wt%, and dimethyl sulfoxide-$d_6$ (DMSO-$d_6$; 99.9% purity) were purchased from Cambridge Isotope Laboratories. All chemicals were used without further purification. Water used in this work was double distilled and filtered through a millipore membrane.

**Analytical techniques.** Elemental microanalyses (EA) were performed by using a LECO CHNS-932 CHNS elemental analyzer (Section 2). Powder X-ray diffraction data for refinement was collected on a Bruker D8 Advance employing Ni filtered Cu Kα (λ = 1.54059 Å) radiation (Section 3). Thermogravimetric analysis (TGA) curves were recorded on a TA Q500 thermal analysis system under airflow (Section 4). Solution $^1H$ NMR spectra were acquired on a Bruker AVB-500 NMR spectrometer (Section 4). Low-pressure $N_2$ adsorption and $CO_2$ measurements were carried out on a Micromeritics 3Flex surface characterization analyzer (Section 4, Section 6). A liquid $N_2$ bath was used for measurements at 77 K. Helium was used as estimation of dead space. Ultrahigh-purity-grade $N_2$ and He (99.999% purity) were used throughout adsorption experiments.

## Section 2: Synthesis of PCN-280, MOF-908, and MOF-909

### Synthesis of 1,3,5-tris(4-carboxyphenyl)benzene ($H_3BTB$) and azobenzene-3,3'-dicarboxylic acid (3,3'-azoBDC):

$H_3BTB$ and 3,3'-azoBDC were synthesized following the reported procedure.[1,2]

### Synthesis of PCN-280:

The synthetic procedure of PCN-280 was slightly modified comparing to the original report.[3] Particularly, a mixture of $Fe(NO_3)_3{\cdot}9H_2O$ (0.03686 g, 0.0912 mmol), 1,3,5-tris(4-carboxyphenyl) benzene ($H_3BTB$) (0.020 g, 0.046 mmol), and biphenyl-4,4′-dicarboxylic acid ($H_2BPDC$) (0.011 g, 0.046 mmol) in *N*,*N*-dimethylformamide (DMF, 3.5 mL) was added to a 8-mL glass vial. The procedure was followed by the addition of 0.5 mL of methanol and 0.2 mL of acetic acid. The mixture was then sonicated for 1 min and isothermally heated at 120 °C for 24 h. The reaction was then cooled down to room temperature and the solid product was obtained. The mother liquor was removed and the solid was washed with DMF (5 × 3 mL, each day) for 3 days. After that, the sample was exchanged solvent by acetone for 3 days (5 × 3 mL, each day). The solvent-exchanged sample was activated by heating at 80 °C under low pressure for 24 h producing 16.4 mg of activated MOF (44 % yield based on $Fe(NO_3)_3{\cdot}9H_2O$).

### Synthesis of MOF-909:

A mixture of $Fe(NO_3)_3{\cdot}9H_2O$ (0.03686 g, 0.0912 mmol), 1,3,5-tris(4-carboxyphenyl) benzene ($H_3BTB$) (0.020 g, 0.046 mmol), and 3,3'-azobenzene dicarboxylic acid (3,3'-AzoBDC) (0.01362 g, 0.050 mmol) in *N*,*N*-dimethylformamide (DMF, 3.5 mL) was added to an 8-mL glass vial. The procedure was followed by the addition of 0.5 mL of methanol and 0.2 mL of acetic acid. The mixture was then sonicated for 1 min and isothermally heated at 120 °C for 24 h. The reaction was then cooled down to room temperature and the solid product is washed with DMF (5 × 3 mL, each day) for 3 days and afterward, the MOF material was exchanged by acetone for 3 days (5 × 3 mL, each day). The solvent-exchanged sample was activated by heating at 100 °C under low pressure for 24 h producing 7.8 mg of activated MOF (21 % yield based on $Fe(NO_3)_3{\cdot}9H_2O$). EA of activated sample: Calcd. for $C_{50}H_{28}N_2O_{16}Fe_3$ = $Fe^{III}_3O(OH)(BTB)_{4/3}$(3,3'-azoBDC): C, 55.59; H, 2.61; N, 2.59%. Found: C, 55.18; H, 2.58; N, 1.87%.

**Synthesis of MOF-908 by reticular control**

*The molar ratio of 3,3'-AzoBDC:$H_2$BPDC = 50:50 mol%*

$Fe(NO_3)_3 \cdot 9H_2O$ (0.03686g, 0.0912mmol), 1,3,5-tris(4-carboxyphenyl) benzene ($H_3$BTB) (0.020 g, 0.046 mmol), 4,4'-biphenyl dicarboxylic ($H_2$BPDC) (0.0055 g, 0.023 mmol), and 3,3'-azobenzene dicarboxylic acid (3,3'-AzoBDC) (0.00681 g, 0.025 mmol) were added in the mixture of *N*,*N*-dimethylformamide (DMF) (3.5 mL), methanol (0.5 mL), and acetic acid (0.2 mL). This mixture was sonicated for 1 min to fully dissolve the reagents. The solution was then introduced to an 8-mL glass vial and heated at 120 °C in an isothermal oven for 24 h. The orange crystalline product was collected after cooling down to room temperature and washed with DMF (5 × 3 mL, each day) for 3 days. After that, the sample was exchanged solvent by acetone for 3 days (5 × 3 mL, each day). Finally, the sample was activated by heating at 100 °C under low pressure for 24 h leading to obtain 20.8 mg of activated MOF (56 % yield based on $Fe(NO_3)_3 \cdot 9H_2O$). EA of activated sample: Calcd. for $C_{50}H_{28}O_{16}Fe_3 \cdot C_3H_7NO$ ($C_3H_7NO$ = DMF) = $Fe^{III}_3O(OH)(BTB)_{4/3}(BPDC) \cdot$DMF: C, 56.56; H, 3.13; N, 1.24%. Found: C, 54.72; H, 3.66; N, 1.64%. Noted: DMF is the guest molecules insided the pores.

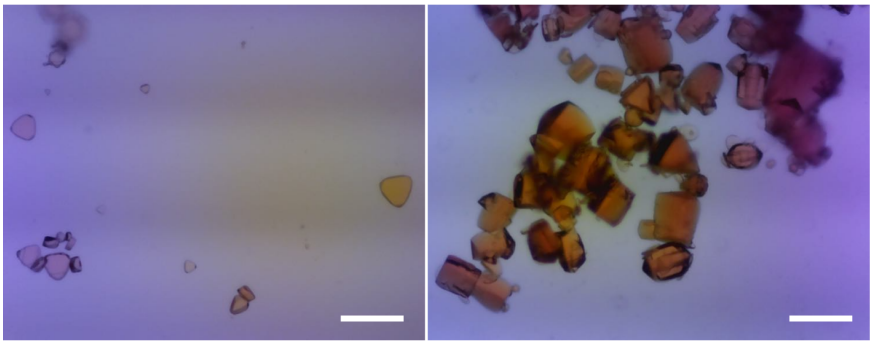


**Figure 1**. The microscope images of PCN-280 single crystals showing the thin hexagonal shape and MOF-908 single crystals which clearly show the thick trigonal prism growing along c direction. Scale bar, 100 μm.

*Investigation of MOF-908 synthesis by systematically schematic procedure*

**Table 1**. The ratio molar of 3,3'-AzoBDC:$H_2$BPDC used for the synthetic investigation at 120 °C

| **$H_3$BTB (mmol)** | **3,3'-AzoBDC:$H_2$BPDC (mol %)** | **Synthetic condition** | **Product** |
|---|---|---|---|
| 0.046 | 100:0 (0.050:0 mmol) | DMF:MeOH:AcOH (3.5:0.5:0.2 mL) | MOF-909 |
| | 90:10 (0.045:0.005 mmol) | | MOF-909 |
| | 80:20 (0.040:0.009 mmol) | | MOF-909 |
| | 70:30 (0.035:0.014 mmol) | | MOF-909 |
| | 60:40 (0.030:0.018 mmol) | | MOF-908 |
| | 50:50 (0.025:0.023 mmol) | | MOF-908 |
| | 40:60 (0.020:0.027 mmol) | | PCN-280 |
| | 30:70 (0.015:0.032 mmol) | | PCN-280 |
| | 20:80 (0.01:0.0364 mmol) | | PCN-280 |
| | 10:90 (0.0005:0.041 mmol) | | PCN-280 |
| | 0:100 (0:0.046 mmol) | | PCN-280 |

## Section 3: Crystal structures refinement of MOF-908 and MOF-909

A structural model of MOF-908 was executed by using the *Materials Visualizer* module of Materials Studio software (*Material Studio* ver. 6.0, Accelrys Software Inc.) Upon completion of the structural model, an energetic minimization was performed using the universal force field implemented in the *Forcite* module of *Materials Studio*. During this process, the unit cell parameters were also optimized until proper convergence was achieved (energy convergence criteria were set at $10^{-4}$ kcal $mol^{-1}$).

A full profile pattern fitting (Pawley and Rietveld then) from $2\theta$ = 4° – 50° (The first peak located at around 3.6 degree 2theta did not occur when long run PXRD measurement was conducted which is due to the preferred orientation) was performed against the experimental powder pattern which was achieved with the satisfactory agreement with the experimental PXRD pattern, as demonstrated by the fitting that converged with reasonable residual values ($R_{wp}$ = 4.23%, $R_p$ = 2.57%) to yield the final unit cell parameters ($a$ = 32.9145 Å). The fractional atomic coordinates and refined cell parameters for MOF-908 can be found in Table 2. Further crystal structure information is provided in Table 3.

MOF-909 structural refinement was performed similar to MOF-908. The converged residual values were found to be 4.93% and 2.78% for $R_{wp}$ and $R_p$, respectively. The fractional atomic coordinates and refined cell parameters for MOF-909 can be found in Table 4. Further crystal structure information is provided in Table 5.

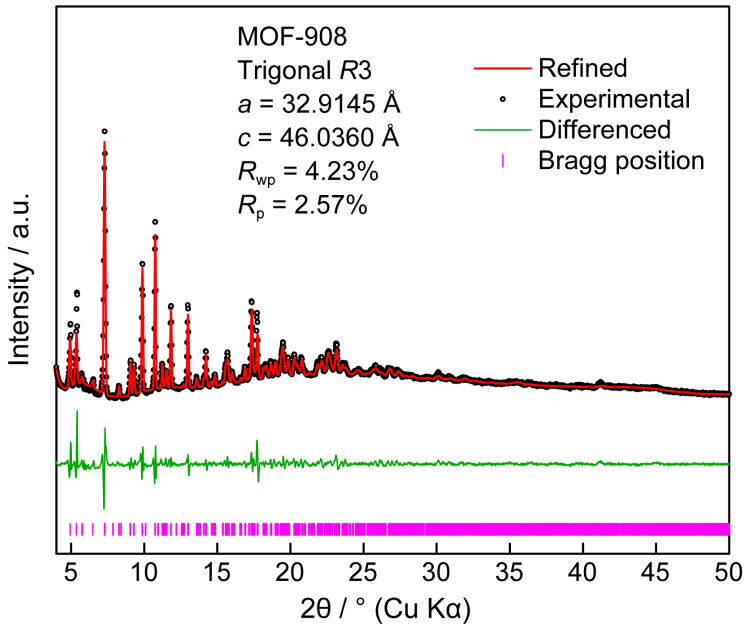


**Figure 2**. PXRD analysis of MOF-908 displaying the experimental pattern (black), refined Rietveld fitting (red). The difference plot (green) and Bragg positions (pink) are also provided.

**Table 2.** Atomic coordinates and refined unit cell parameters of MOF-908.

| **Name** | MOF-908 | | | |
|---|---|---|---|---|
| **Space Group** | *R*3 (No. 146) | | | |
| ***a* (Å)** | 32.9145 | | | |
| **Unit Cell Volume (Å$^3$)** | 43191.9 | | | |
| **Atom Name** | Occupancy | *x* | *y* | *z* |
| C1 | 1 | 0.0573 | 0.251 | 0.9985 |
| C2 | 1 | 0.9953 | 0.1802 | 0.9716 |
| C3 | 1 | 0.0109 | 0.2066 | 0.9972 |
| C4 | 1 | 0.9822 | 0.1896 | 0.0219 |
| C5 | 1 | 0.9393 | 0.1471 | 0.0211 |
| C6 | 1 | 0.9238 | 0.1204 | 0.9956 |
| C7 | 1 | 0.9522 | 0.1377 | 0.9708 |
| C8 | 1 | 0.7508 | 0.9386 | 0.9964 |
| C9 | 1 | 0.7973 | 0.0242 | 0.0108 |
| C10 | 1 | 0.7945 | 0.9855 | 0.9956 |
| C11 | 1 | 0.8342 | 0.9919 | 0.98 |
| C12 | 1 | 0.8759 | 0.0357 | 0.9798 |
| C13 | 1 | 0.8789 | 0.0743 | 0.9951 |
| C14 | 1 | 0.839 | 0.068 | 0.0105 |
| C15 | 1 | 0.2525 | 0.3711 | 0.9722 |
| C16 | 1 | 0.2939 | 0.4038 | 0.9545 |
| C17 | 1 | 0.339 | 0.4283 | 0.967 |
| C18 | 1 | 0.3776 | 0.4618 | 0.9511 |
| C19 | 1 | 0.372 | 0.4723 | 0.9225 |
| C20 | 1 | 0.3268 | 0.4469 | 0.9098 |
| C21 | 1 | 0.2883 | 0.4128 | 0.9256 |
| C22 | 1 | 0.4127 | 0.5103 | 0.9064 |
| C23 | 1 | 0.4466 | 0.5513 | 0.9208 |
| C24 | 1 | 0.4855 | 0.5872 | 0.906 |
| C25 | 1 | 0.4898 | 0.5825 | 0.8763 |
| C26 | 1 | 0.4566 | 0.5419 | 0.8614 |
| C27 | 1 | 0.4182 | 0.5059 | 0.8766 |
| C28 | 1 | 0.4635 | 0.5364 | 0.8302 |
| C29 | 1 | 0.4247 | 0.5141 | 0.8113 |
| C30 | 1 | 0.4315 | 0.5081 | 0.7822 |
| C31 | 1 | 0.4773 | 0.5249 | 0.7713 |
| C32 | 1 | 0.516 | 0.5479 | 0.79 |
| C33 | 1 | 0.5092 | 0.5532 | 0.8191 |
| C34 | 1 | 0.4851 | 0.5163 | 0.741 |
| C35 | 1 | 0.5226 | 0.6289 | 0.9218 |
| C36 | 1 | 0.539 | 0.6231 | 0.9486 |
| C37 | 1 | 0.5744 | 0.662 | 0.9634 |
| C38 | 1 | 0.5943 | 0.7077 | 0.9516 |
| C39 | 1 | 0.5781 | 0.7135 | 0.9247 |
| C40 | 1 | 0.5427 | 0.6745 | 0.9099 |
| C41 | 1 | 0.6298 | 0.7492 | 0.9681 |

| | | | | |
|---|---|---|---|---|
| C42 | 1 | 0.2032 | 0.4174 | 0.0436 |
| C43 | 1 | 0.2282 | 0.4677 | 0.0522 |
| C44 | 1 | 0.2142 | 0.4984 | 0.0405 |
| C45 | 1 | 0.2388 | 0.5464 | 0.047 |
| C46 | 1 | 0.2777 | 0.5649 | 0.0659 |
| C47 | 1 | 0.291 | 0.534 | 0.0782 |
| C48 | 1 | 0.2668 | 0.4858 | 0.0713 |
| C49 | 1 | 0.306 | 0.6169 | 0.0706 |
| C50 | 1 | 0.284 | 0.6444 | 0.0711 |
| Fe1 | 1 | 0.2171 | 0.3374 | 0.029 |
| Fe2 | 1 | 0.1505 | 0.3029 | 0.97 |
| Fe3 | 1 | 0.116 | 0.3377 | 0.0272 |
| H1 | 1 | 0.9932 | 0.2089 | 0.0421 |
| H2 | 1 | 0.941 | 0.1183 | 0.9507 |
| H3 | 1 | 0.8334 | 0.9629 | 0.9683 |
| H4 | 1 | 0.84 | 0.0972 | 0.0222 |
| H5 | 1 | 0.3446 | 0.4218 | 0.9891 |
| H6 | 1 | 0.412 | 0.4796 | 0.9614 |
| H7 | 1 | 0.321 | 0.4543 | 0.888 |
| H8 | 1 | 0.2538 | 0.3947 | 0.9155 |
| H9 | 1 | 0.4424 | 0.5558 | 0.9435 |
| H10 | 1 | 0.5196 | 0.6105 | 0.8649 |
| H11 | 1 | 0.3935 | 0.4738 | 0.8656 |
| H12 | 1 | 0.389 | 0.5013 | 0.819 |
| H13 | 1 | 0.401 | 0.4903 | 0.7682 |
| H14 | 1 | 0.5518 | 0.5606 | 0.7824 |
| H15 | 1 | 0.5399 | 0.5695 | 0.8331 |
| H16 | 1 | 0.5247 | 0.5883 | 0.9581 |
| H17 | 1 | 0.5859 | 0.6562 | 0.9841 |
| H18 | 1 | 0.5923 | 0.7483 | 0.9152 |
| H19 | 1 | 0.5305 | 0.6802 | 0.8894 |
| H20 | 1 | 0.185 | 0.4856 | 0.0254 |
| H21 | 1 | 0.2283 | 0.5692 | 0.0364 |
| H22 | 1 | 0.3205 | 0.547 | 0.0931 |
| H23 | 1 | 0.2781 | 0.4629 | 0.0808 |
| H24 | 1 | 0.2458 | 0.6272 | 0.0701 |
| H25 | 1 | 0.0164 | 0.1923 | 0.9522 |
| H26 | 1 | 0.7674 | 0.0205 | 0.0229 |
| H27 | 1 | 0.1989 | 0.4509 | 0.7074 |
| H28 | 1 | 0.2942 | 0.5337 | 0.6348 |
| H29 | 1 | 0.5132 | 0.547 | 0.598 |
| O1 | 1 | 0.1612 | 0.3257 | 0.0087 |
| O2 | 1 | 0.0685 | 0.2748 | 0.0217 |
| O3 | 1 | 0.084 | 0.2639 | 0.9763 |
| O4 | 1 | 0.7489 | 0.9059 | 0.9807 |
| O5 | 1 | 0.7169 | 0.9327 | 0.0128 |
| O6 | 1 | 0.1392 | 0.2798 | 0.9313 |
| O7 | 1 | 0.2558 | 0.3763 | 0.9993 |

| | | | | |
|---|---|---|---|---|
| O8 | 1 | 0.2154 | 0.3395 | 0.9597 |
| O9 | 1 | 0.4508 | 0.4851 | 0.7266 |
| O10 | 1 | 0.5267 | 0.5393 | 0.7308 |
| O11 | 1 | 0.6458 | 0.7901 | 0.9575 |
| O12 | 1 | 0.643 | 0.7426 | 0.9926 |
| O13 | 1 | 0.1621 | 0.4007 | 0.0331 |
| O14 | 1 | 0.2236 | 0.393 | 0.0469 |

**Table 3.** Important crystallographic information for MOF-908

| **Parameters** | **MOF-908** |
|---|---|
| Empirical formula | $C_{50}Fe_3H_{28}O_{16}$ |
| Calculated density (g $cm^{-3}$) (dried solid) | 0.3534 |
| Symmetry | Trigonal |
| Space group | *R*3 |
| *a* (Å) | 32.9145 |
| *c* (Å) | 46.0360 |
| Unit Cell Volume ($Å^3$) | 43191.9 |
| *Z* | 4 |
| Wavelength (λ, synchrotron) | 1.5406 |
| Temperature (K) | 298 |
| Angular range 2$\theta$ (°) | 4 – 50 |

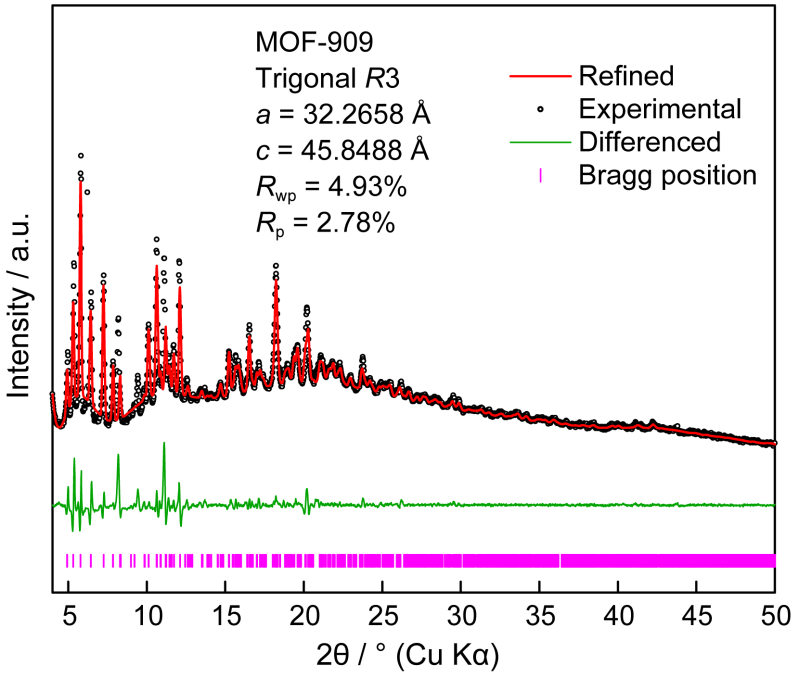


**Figure 3**. PXRD analysis of MOF-909 displaying the experimental pattern (black), refined Rietveld fitting (red). The difference plot (green) and Bragg positions (pink) are also provided.

**Table 4.** Atomic coordinates and refined unit cell parameters of MOF-909.

| **Name** | MOF-909 | | | |
|---|---|---|---|---|
| **Space Group** | *R*3 (No. 146) | | | |
| ***a* (Å)** | 32.2658 | | | |
| ***c* (Å)** | 45.8488 | | | |
| **Unit Cell Volume (Å$^3$)** | 43939.4 | | | |
| **Atom Name** | Occupancy | *x* | *y* | *z* |
| C1 | 1 | 0.0907 | 0.2466 | 0.993 |
| C2 | 1 | 0.0628 | 0.1673 | 0.9733 |
| C3 | 1 | 0.0532 | 0.1982 | 0.9886 |
| C4 | 1 | 0.0078 | 0.1828 | 0.9987 |
| C5 | 1 | 0.9723 | 0.1372 | 0.9928 |
| C6 | 1 | 0.9827 | 0.1066 | 0.9777 |
| C7 | 1 | 0.0278 | 0.1217 | 0.9681 |
| C8 | 1 | 0.7283 | 0.9572 | 0.005 |
| C9 | 1 | 0.7538 | 0.038 | 0.0221 |
| C10 | 1 | 0.7646 | 0.0066 | 0.0084 |
| C11 | 1 | 0.8105 | 0.0223 | 0.9994 |
| C12 | 1 | 0.8453 | 0.0684 | 0.0045 |
| C13 | 1 | 0.8338 | 0.0993 | 0.0182 |
| C14 | 1 | 0.7882 | 0.084 | 0.0267 |
| C15 | 1 | 0.277 | 0.391 | 0.9802 |
| C16 | 1 | 0.315 | 0.4285 | 0.963 |
| C17 | 1 | 0.3582 | 0.4588 | 0.9757 |

| | | | | |
|---|---|---|---|---|
| C18 | 1 | 0.3938 | 0.4934 | 0.9586 |
| C19 | 1 | 0.3864 | 0.499 | 0.9287 |
| C20 | 1 | 0.3425 | 0.4693 | 0.9164 |
| C21 | 1 | 0.3075 | 0.4342 | 0.9332 |
| C22 | 1 | 0.4241 | 0.5348 | 0.9099 |
| C23 | 1 | 0.4573 | 0.5779 | 0.9217 |
| C24 | 1 | 0.4931 | 0.6114 | 0.9041 |
| C25 | 1 | 0.4947 | 0.6023 | 0.874 |
| C26 | 1 | 0.4622 | 0.5592 | 0.8618 |
| C27 | 1 | 0.4275 | 0.5257 | 0.88 |
| C28 | 1 | 0.4659 | 0.5477 | 0.8305 |
| C29 | 1 | 0.4259 | 0.5187 | 0.8138 |
| C30 | 1 | 0.4297 | 0.5052 | 0.7852 |
| C31 | 1 | 0.4735 | 0.521 | 0.7724 |
| C32 | 1 | 0.5134 | 0.5509 | 0.7888 |
| C33 | 1 | 0.5097 | 0.5638 | 0.8175 |
| C34 | 1 | 0.4784 | 0.5061 | 0.7426 |
| C35 | 1 | 0.5308 | 0.6541 | 0.9178 |
| C36 | 1 | 0.5519 | 0.6504 | 0.9436 |
| C37 | 1 | 0.5868 | 0.6899 | 0.9573 |
| C38 | 1 | 0.6015 | 0.7344 | 0.9458 |
| C39 | 1 | 0.5809 | 0.7382 | 0.9196 |
| C40 | 1 | 0.5461 | 0.6983 | 0.9056 |
| C41 | 1 | 0.6352 | 0.7758 | 0.9627 |
| C42 | 1 | 0.203 | 0.4189 | 0.0436 |
| C43 | 1 | 0.2237 | 0.4691 | 0.0497 |
| C44 | 1 | 0.2105 | 0.4965 | 0.0333 |
| C45 | 1 | 0.2359 | 0.545 | 0.0356 |
| C46 | 1 | 0.2747 | 0.5667 | 0.0544 |
| C47 | 1 | 0.2861 | 0.5391 | 0.0719 |
| C48 | 1 | 0.2609 | 0.4909 | 0.0696 |
| C49 | 1 | 0.3046 | 0.618 | 0.0547 |
| C50 | 1 | 0.285 | 0.6468 | 0.0547 |
| Fe1 | 1 | 0.2347 | 0.3522 | 0.0357 |
| Fe2 | 1 | 0.1846 | 0.3109 | 0.9712 |
| Fe3 | 1 | 0.1288 | 0.3328 | 0.023 |
| H1 | 1 | 0.9998 | 0.2064 | 0.0103 |
| H2 | 1 | 0.9559 | 0.0713 | 0.973 |
| H3 | 1 | 0.0356 | 0.098 | 0.9564 |
| H4 | 1 | 0.8197 | 0.9986 | 0.9891 |
| H5 | 1 | 0.8601 | 0.135 | 0.0222 |
| H6 | 1 | 0.7795 | 0.1079 | 0.0373 |
| H7 | 1 | 0.3648 | 0.455 | 0.9987 |
| H8 | 1 | 0.4273 | 0.5152 | 0.9688 |
| H9 | 1 | 0.3349 | 0.4733 | 0.8937 |
| H10 | 1 | 0.2741 | 0.412 | 0.923 |
| H11 | 1 | 0.4554 | 0.5856 | 0.9447 |
| H12 | 1 | 0.5221 | 0.6285 | 0.8604 |

| | | | | |
|---|---|---|---|---|
| H13 | 1 | 0.404 | 0.4916 | 0.8712 |
| H14 | 1 | 0.3916 | 0.5064 | 0.8229 |
| H15 | 1 | 0.3984 | 0.4825 | 0.7731 |
| H16 | 1 | 0.5477 | 0.5634 | 0.7796 |
| H17 | 1 | 0.5413 | 0.5852 | 0.8297 |
| H18 | 1 | 0.5413 | 0.6167 | 0.9532 |
| H19 | 1 | 0.6016 | 0.6855 | 0.9775 |
| H20 | 1 | 0.5911 | 0.772 | 0.9103 |
| H21 | 1 | 0.5303 | 0.7019 | 0.8856 |
| H22 | 1 | 0.1822 | 0.4807 | 0.0176 |
| H23 | 1 | 0.2264 | 0.5654 | 0.0217 |
| H24 | 1 | 0.3151 | 0.5549 | 0.087 |
| H25 | 1 | 0.2717 | 0.4707 | 0.0827 |
| H26 | 1 | 0.2476 | 0.6313 | 0.0545 |
| H27 | 1 | 0.0976 | 0.1783 | 0.9654 |
| H28 | 1 | 0.7187 | 0.0269 | 0.0292 |
| H29 | 1 | 0.4759 | 0.4999 | 0.599 |
| N1 | 1 | 0.9258 | 0.1231 | 0.0017 |
| N2 | 1 | 0.892 | 0.0827 | 0.9961 |
| O1 | 1 | 0.1826 | 0.3314 | 0.0101 |
| O2 | 1 | 0.0917 | 0.2684 | 0.0163 |
| O3 | 1 | 0.1208 | 0.2647 | 0.9725 |
| O4 | 1 | 0.7339 | 0.9321 | 0.9862 |
| O5 | 1 | 0.6927 | 0.9419 | 0.0215 |
| O6 | 1 | 0.186 | 0.29 | 0.9323 |
| O7 | 1 | 0.274 | 0.3962 | 0.0076 |
| O8 | 1 | 0.2482 | 0.3548 | 0.9663 |
| O9 | 1 | 0.4453 | 0.4693 | 0.7315 |
| O10 | 1 | 0.5169 | 0.5303 | 0.7293 |
| O11 | 1 | 0.6441 | 0.8161 | 0.9551 |
| O12 | 1 | 0.6541 | 0.7693 | 0.985 |
| O13 | 1 | 0.165 | 0.3974 | 0.0295 |
| O14 | 1 | 0.2253 | 0.3992 | 0.0522 |

**Table 5.** Important crystallographic information for MOF-909

| **Parameters** | **MOF-909** |
|---|---|
| Empirical formula | $C_{50}Fe_3H_{28}O_{16}N_2$ |
| Calculated density (g $cm^{-3}$) (dried solid) | 0.3569 |
| Symmetry | Trigonal |
| Space group | *R*3 |
| *a* (Å) | 32.2658 |
| *c* (Å) | 45.8488 |
| Unit Cell Volume ($Å^3$) | 43939.4 |
| *Z* | 4 |
| Wavelength (λ, synchrotron) | 1.5406 |
| Temperature (K) | 298 |
| Angular range 2$\theta$ (°) | 4 – 50 |

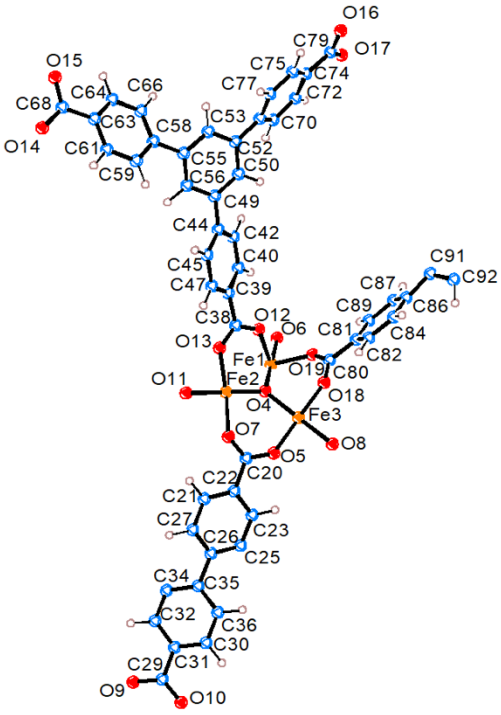


**Figure 4**. The asymmetric unit of MOF-908. The unit was drawn by ORTEP with thermal ellipsoids style at 50% probability. The labels for hydrogen atoms (pink) were omitted for clarity.

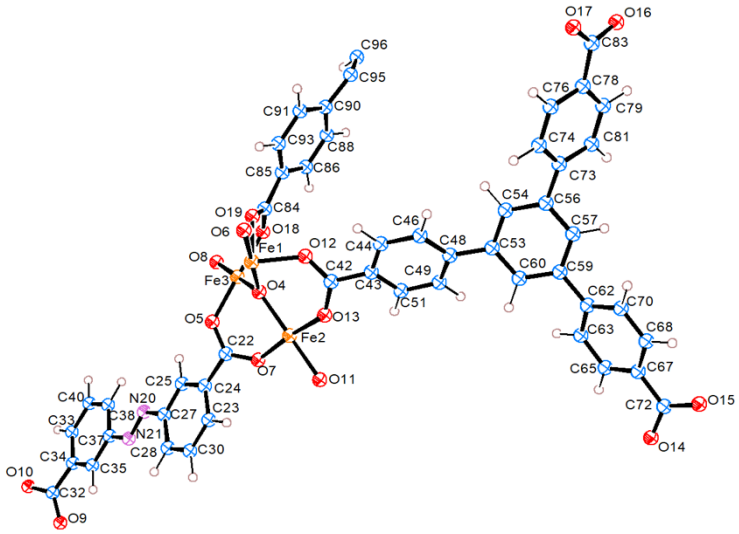


**Figure 5**. The asymmetric unit of MOF-909. The unit was drawn by ORTEP with thermal ellipsoids style at 50% probability. The labels for hydrogen atoms (pink) were omitted for clarity.

## Section 4: Structural characterization of MOF-908 and MOF-909

*PXRD analysis*

PXRD data was collected using a Bruker D8 Advance diffractometer in reflectance Bragg-Brentano geometry employing Ni filtered Cu Kα focused radiation (1.54059 Å, 1.54439 Å) at 1600 W (40 kV, 40 mA) power. The PXRD instrument is equipped with a LynxEye detector. The best counting statistics were achieved by collecting samples using a 0.02° 2θ step scan from 3 – 30° with exposure time of 0.5 s per step. The measurement was performed at room temperature and atmospheric pressure.

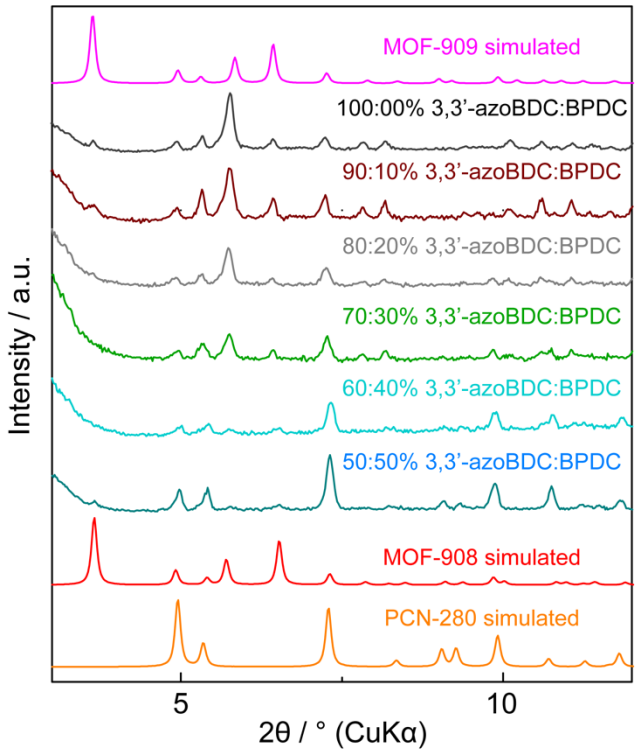


**Figure 6**. PXRD analyses of MOF-908 synthesized by reticular control and MOF-909. The first peak (101) of MOF-908 is low intensity due to the preferred orientation which can be enhanced after activation (see Figure 7).

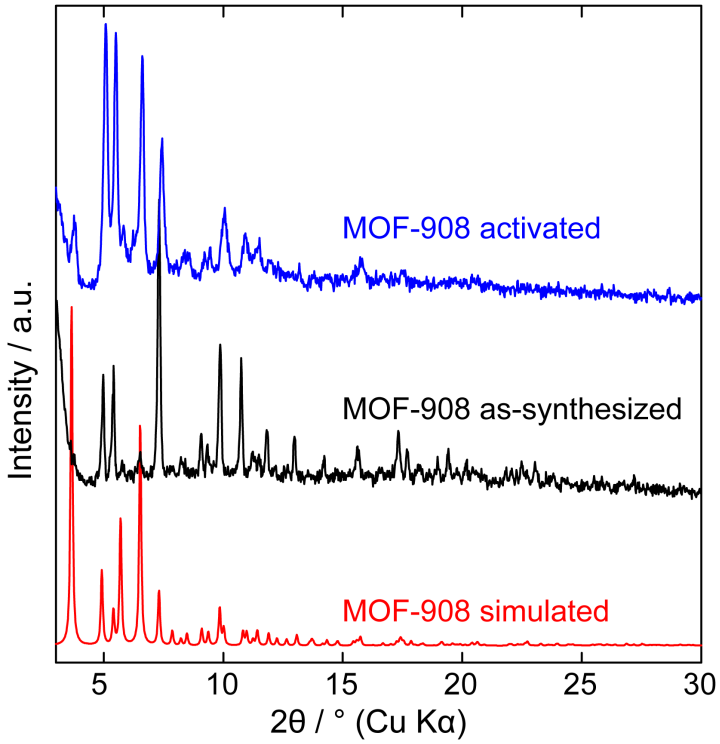


**Figure 7**. PXRD of simulated MOF-908 compared to as-synthesized and activated PXRD patterns.

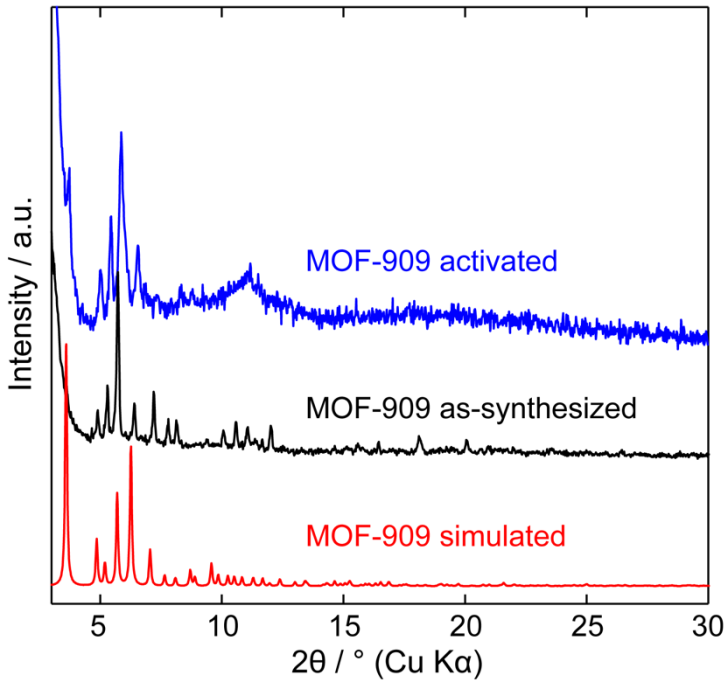


**Figure 8**. PXRD of simulated MOF-909 compared to as-synthesized and activated PXRD patterns.

*Thermogravimetric analysis*

The thermal stability of MOF-908 and MOF-909 was examined by thermogravimetric analysis. In this measurement, an activated sample of MOF (12 mg) was heated under air flow (60 mL $min^{-1}$) from 30 to 600 °C with a gradient of 5 °C $min^{-1}$.

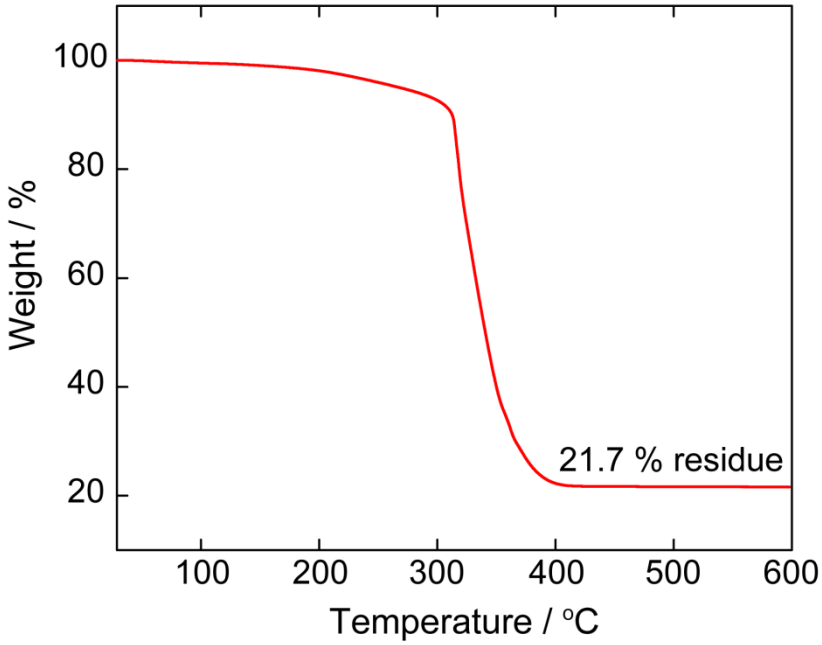


**Figure 9**. Thermogravimetric analysis of activated MOF-908 under air flow.

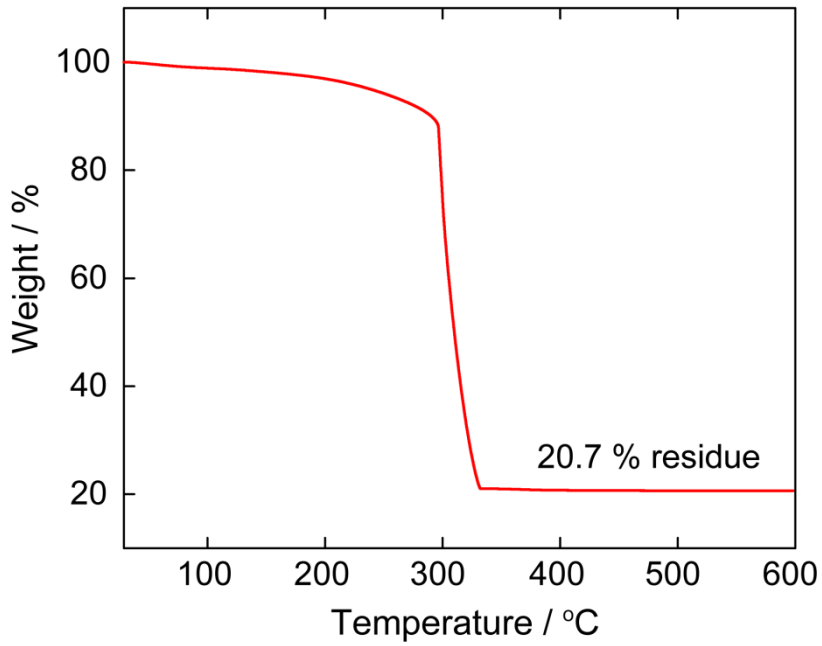


**Figure 10**. Thermogravimetric analysis of activated MOF-909 under air flow.

**Table 6**. Measured and calculated values of weight loss during heating of MOF-908 and MOF-909 under airflow

| Assignment | Composition | Weight loss (%) | | | |
|---|---|---|---|---|---|
| | | MOF-908 | | MOF-909 | |
| | | Measured | Calculated | Measured | Calculated |
| Linker | Linker | 78.3 | 77.2 | 79.3 | 77.8 |
| Residue | $Fe_2O_3$ | 21.7 | 22.8 | 20.7 | 22.2 |

The mass loss of the experiment by the TGA curve is consistent with the calculated value generated from the structural formula of MOFs.

*$N_2$ adsorption isotherm*

The permanent porosity of activated MOF-908, MOF-909, and PCN-280 were proven by $N_2$ adsorption at 77 K, measured by a Micromeritics 3Flex surface characterization analyzer.

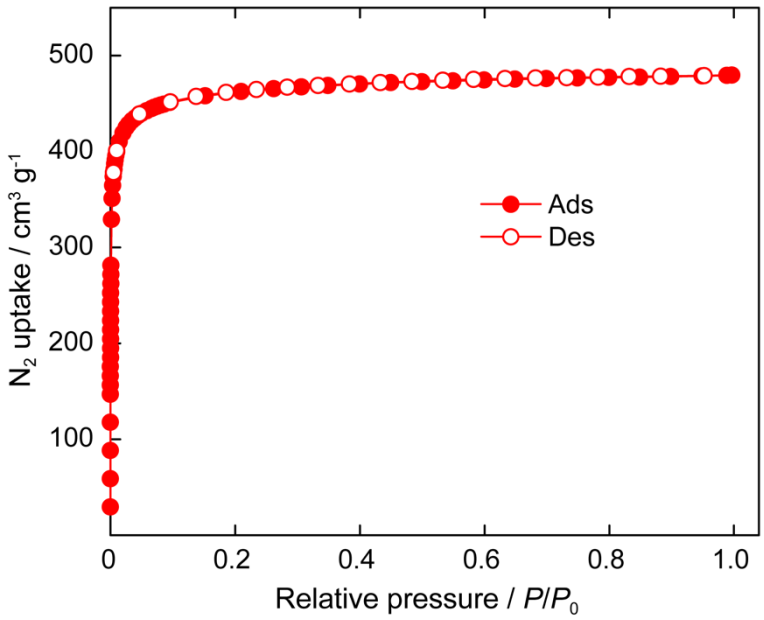


**Figure 11**. $N_2$ sorption isotherms of activated MOF-908 at 77 K. The filled and open circles represent the adsorption and desorption branches, respectively. The connecting line is provided as a guide for the eyes.

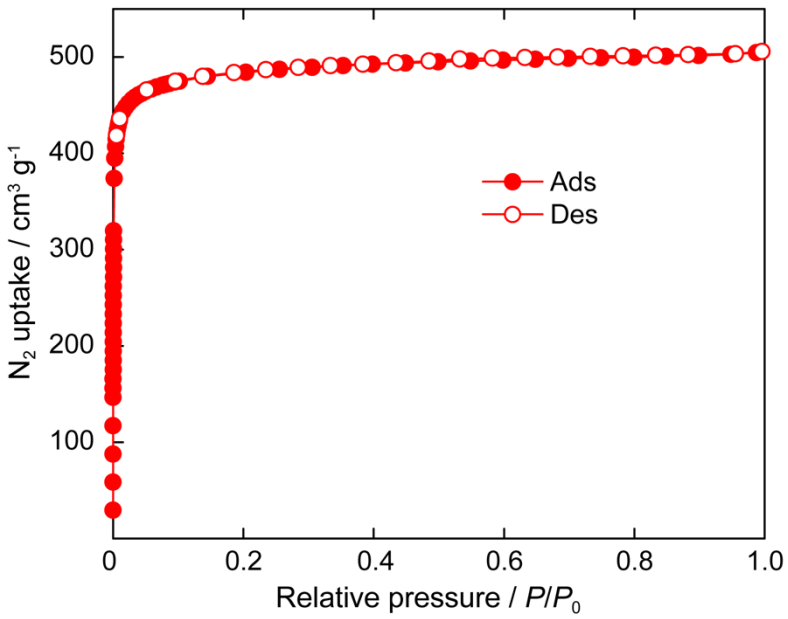


**Figure 12**. $N_2$ sorption isotherms of activated MOF-909 at 77 K. The filled and open circles represent the adsorption and desorption branches, respectively. The connecting line is provided as a guide for the eyes.

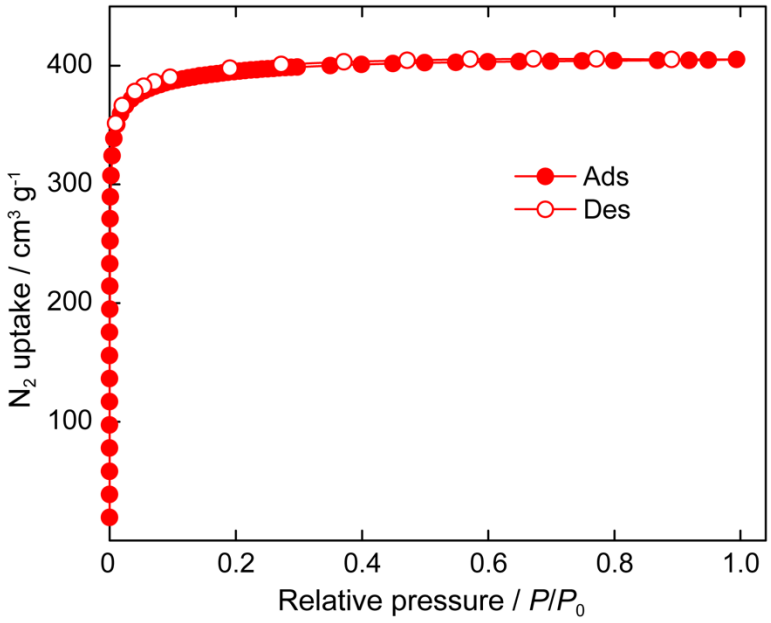


**Figure 13**. $N_2$ sorption isotherms of activated PCN-280 at 77 K. The filled and open circles represent the adsorption and desorption branches, respectively. The connecting line is provided as a guide for the eyes.

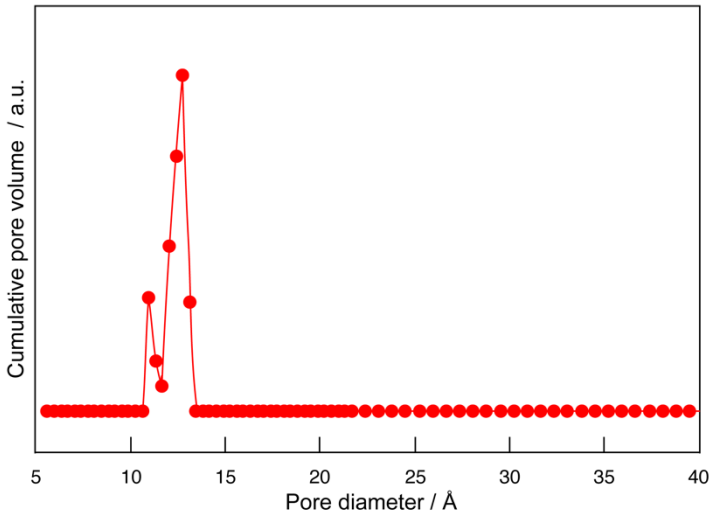


**Figure 14**. Pores size distribution of PCN-280 based on DFT calculation from the $N_2$ adsorption isotherm.

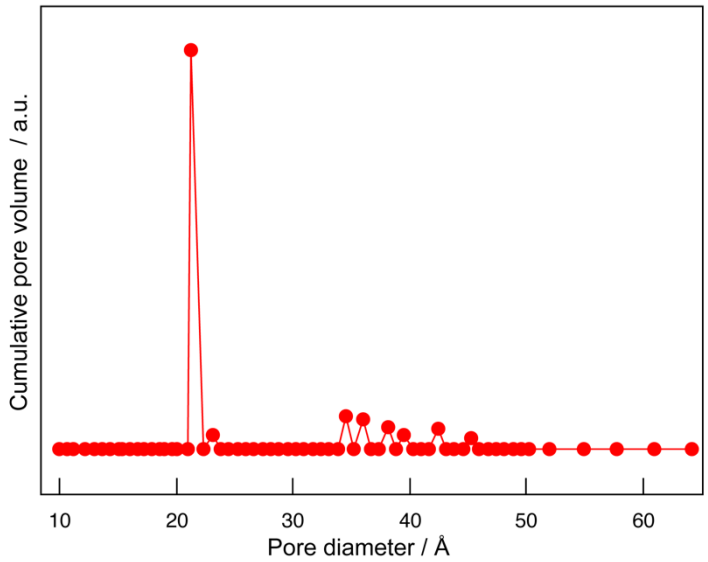


**Figure 15**. Pores size distribution of MOF-908 based on DFT calculation from the $N_2$ adsorption isotherm.

**Table 7**. Comparison of porosity of MOF-908, MOF-909, and PCN-280

| Material | BET ($m^2$ $g^{-1}$) | Langmuir ($m^2$ $g^{-1}$) | Theoretical value ($m^2$ $g^{-1}$) |
|---|---|---|---|
| PCN-280 | 1500 | 1750 | 1800 |
| MOF-908 | 1850 | 2315 | 2300 |
| MOF-909 | 1945 | 2430 | 2350 |

*Nuclear magnetic resonance (NMR) spectroscopy*

An activated sample (7 mg) of MOF-908 (50:50 mol%, or 60:40 mol%) or MOF-909 (70:30 mol% or 100:0 mol%) was digested by 40 wt% of NaOD/$D_2O$ (10 µL) and 600 µL of $D_2O$. The mixure was sonicated 15 minutes to fully dissolve the linkers. The ratio of BTB over BPDC is 4/3 over 1 was found in MOF-908. The similar ratio (4/3:1) of BTB over 3,3'-azoBDC is also obtained.

$^1$H-NMR of MOF-908 (500 MHz, NaOD/$D_2O$): δ = 7.29 (s, 3.0H, $BTB^{3-}$), 7.25 (d, 6.0H, $BTB^{3-}$), 7.69 (d, 6.0H, $BTB^{3-}$), 7.59 (d, 3.0H, $BPDC^{2-}$), 7.80 (d, 3.0H, $BPDC^{2-}$) ppm.

$^1$H-NMR of MOF-909 (500 MHz, NaOD/$D_2O$): δ = 7.29 (s, 3.0H, $BTB^{3-}$), 7.25 (d, 6.0H, $BTB^{3-}$), 7.69 (d, 6.0H, $BTB^{3-}$), 8.35 (s, 1.5H, 3,3'-$azoBDC^{2-}$), 8.15 (s, 1.5H, 3,3'-$azoBDC^{2-}$), 7.95 (s, 1.5H, 3,3'-$azoBDC^{2-}$), 7.90 (s, 1.5H, 3,3'-$azoBDC^{2-}$) ppm.

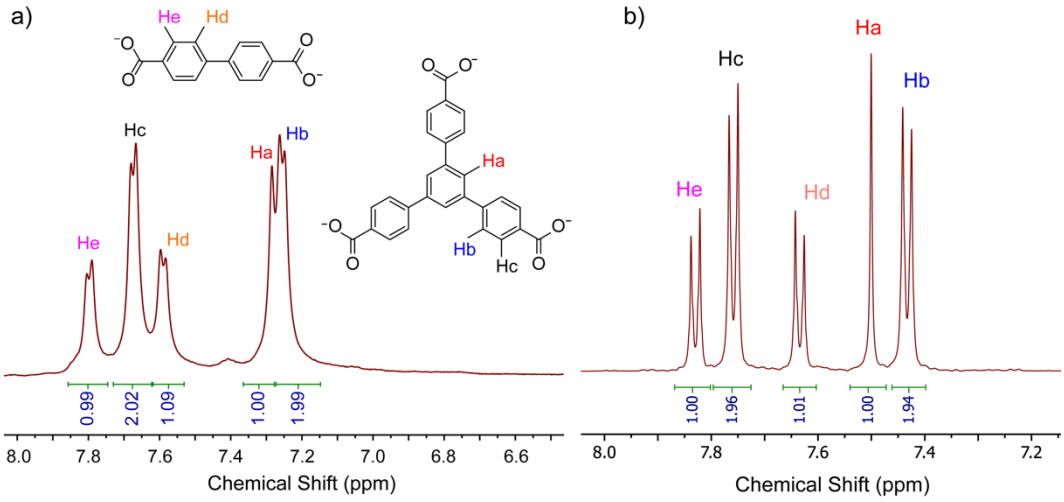


**Figure 16**. $^1$H-NMR analysis of activated MOF-908 (a) compared to PCN-280 (b) displaying the same ratio of mixed linkers (BTB and BPDC). The chemical shift had been shifted on left side for PCN-280.

*Mechanical stability test of MOF-908 and MOF-909*

MOF-908 and MOF-909 were washed with acetone for 3 d. The PXRD analyses were then collected for the pelleted samples (13 mm diameter, pressed from 1 to 11 tons $cm^{-2}$).

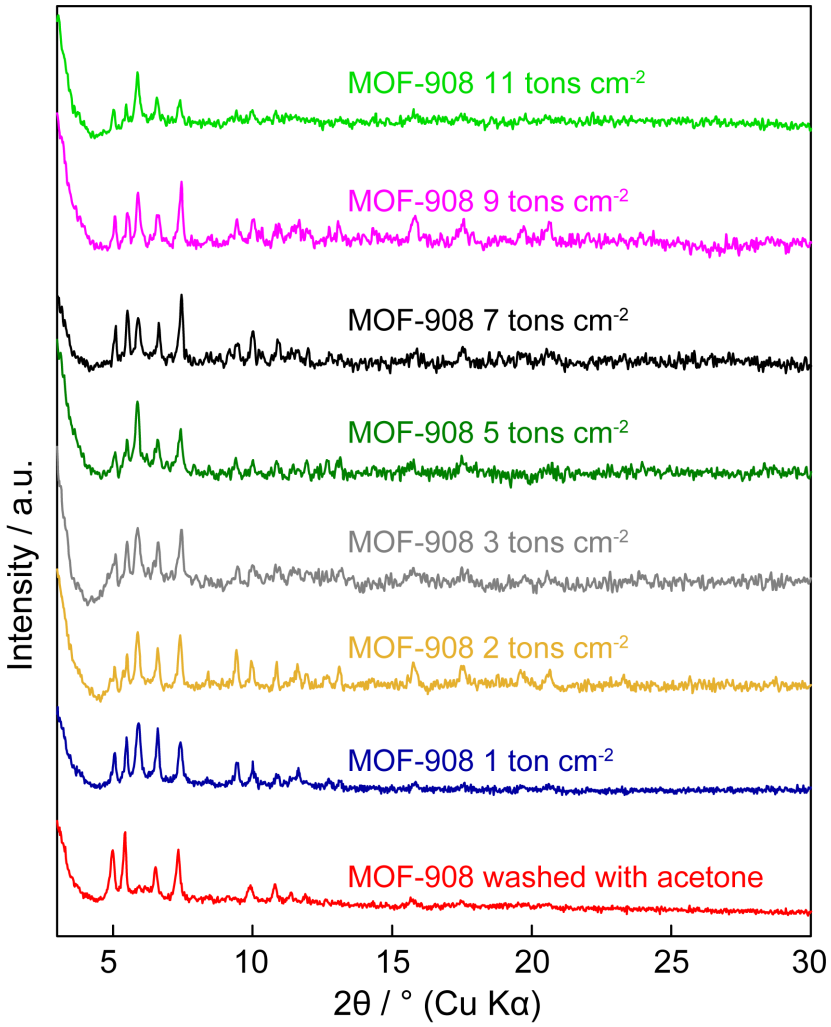


**Figure 17**. PXRD analysis of pelleted MOF-908 displaying the high mechanical stability up to 11 tons $cm^{-2}$.

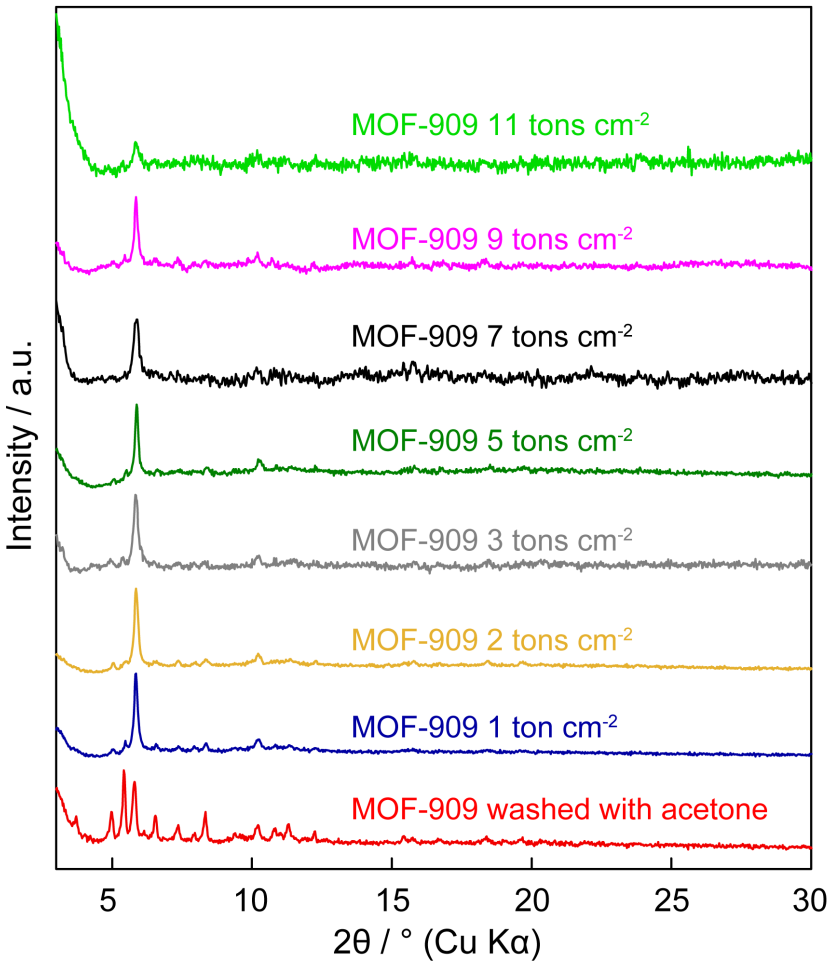


**Figure 18**. PXRD analysis of pelleted MOF-909 displaying the low mechanical stability up to 5 tons $cm^{-2}$.

## Section 5: Topological analysis

The topology of MOF-908 and MOF-909 was analyzed by ToposPro software[4] which showed the new topology and named **nht**. Since it was new, the net was deposited in the RCSR database.[5] $Fe_3O(OH)(CO_2)_6$ cluster and organic linkers: $BTB^{3-}$ and $BPDC^{2-}$ or 3,3'-$azoBDC^{2-}$ were simplified as nodes. A trinodal net containing (3,3,6)-connected points of extension was found in **nht** network with the *pqrs* transitivity of *3553*. Natural tilings of those of MOFs were analyzed by 3dt software.[5]

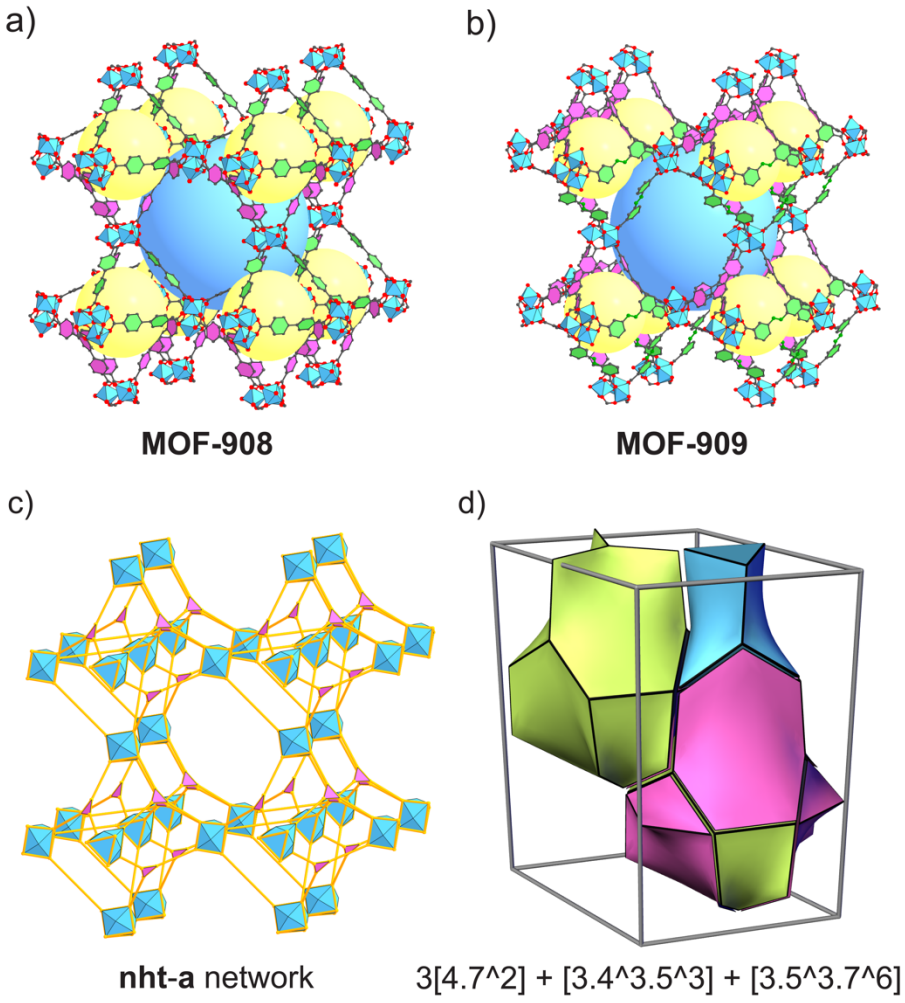


**Figure 19**. The 3D crystal structure of MOF-908 (a) and MOF-909 (b) which were simplified to form the augmented net (c). The natural tiling of MOF-908 and MOF-909 is $3[4.7^2] + 3[4^3.5^3] + [3.5^3.7^6]$ (d).

## Section 6: Gas uptake study

*$CO_2$ adsorption study*

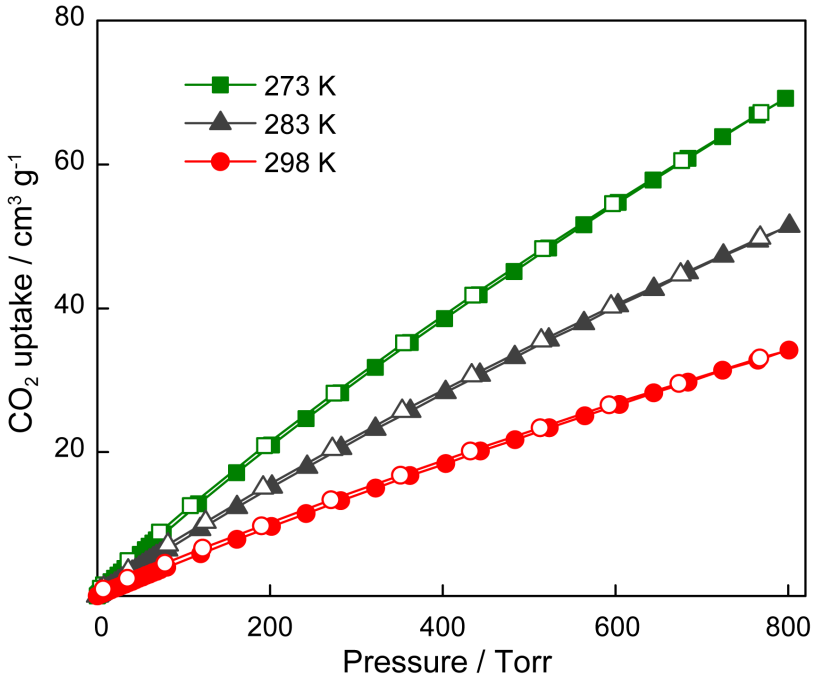


**Figure 20.** Low-pressure $CO_2$ adsorption isotherms for MOF-908 measured at 278, 288, and 298 K

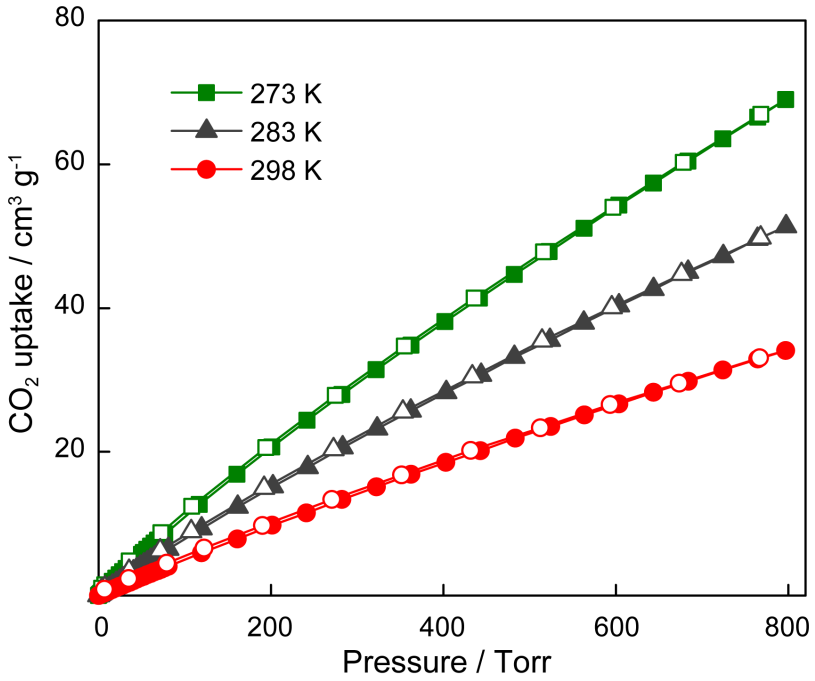


**Figure 21.** Low-pressure $CO_2$ adsorption isotherms for MOF-909 measured at 278, 288, and 298 K

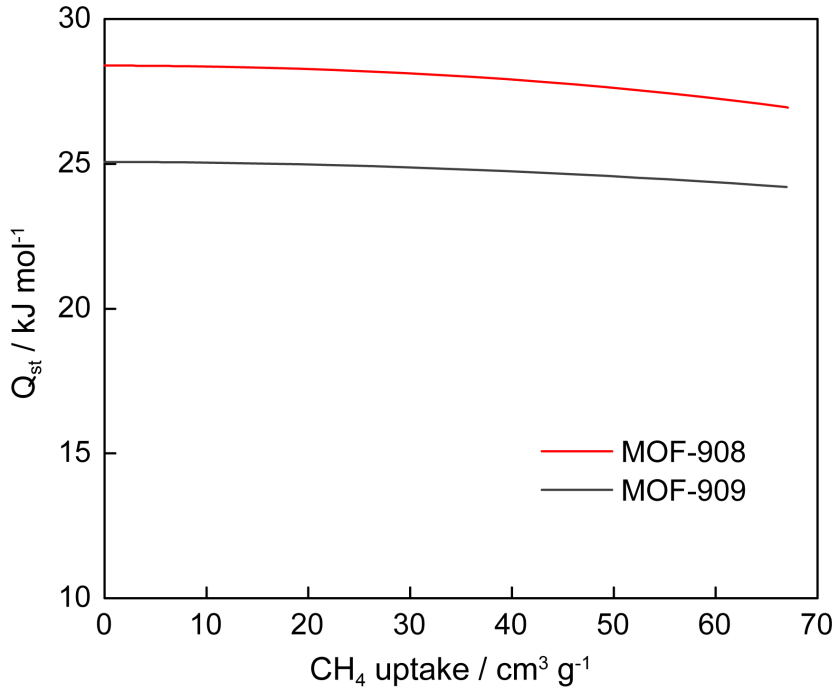


**Figure 22.** Isosteric heat of adsorption of MOF-908 and MOF-909.

*$CH_4$ uptake at low pressure for PCN-280*

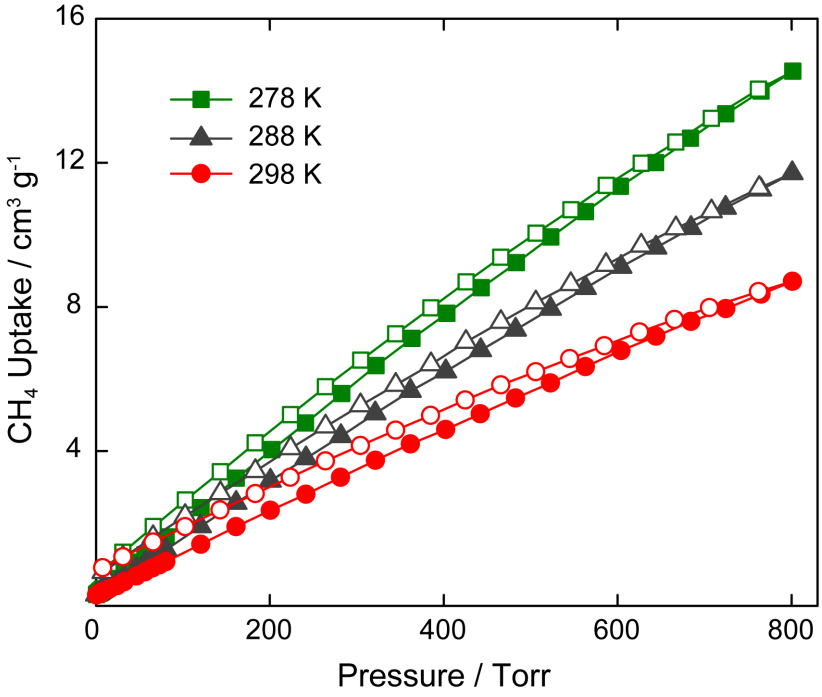


**Figure 23.** Low-pressure $CH_4$ adsorption isotherms for PCN-280 measured at 278, 288, and 298 K.

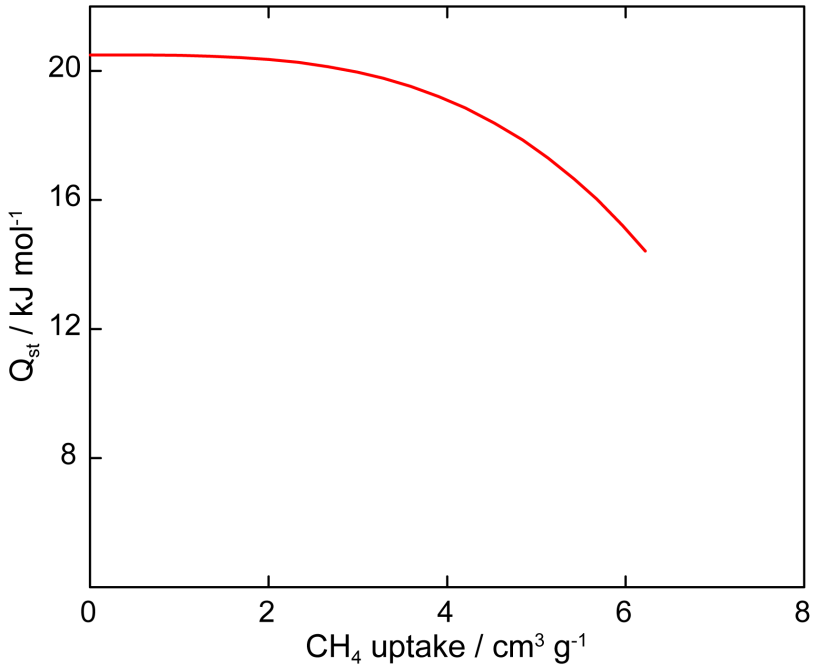


**Figure 24.** Isosteric enthalpies of adsorption for PCN-280.

*$CH_4$ uptake at high pressure for PCN-280*

High pressure $CH_4$ adsorption isotherms in the range of 0-85 bar were recorded on a Hiden Isochema IMI-135 system. In a measurement, activated sample was weighed loaded into a stainless steel sample holder inside an inert atmosphere glovebox. Prior to connecting the sample holder to the VCR fittings of the complete high-pressure assembly, a known amount of glass wool (d = 2.06 g cm$^{-3}$) was tightly packed on the top of the sample holder.

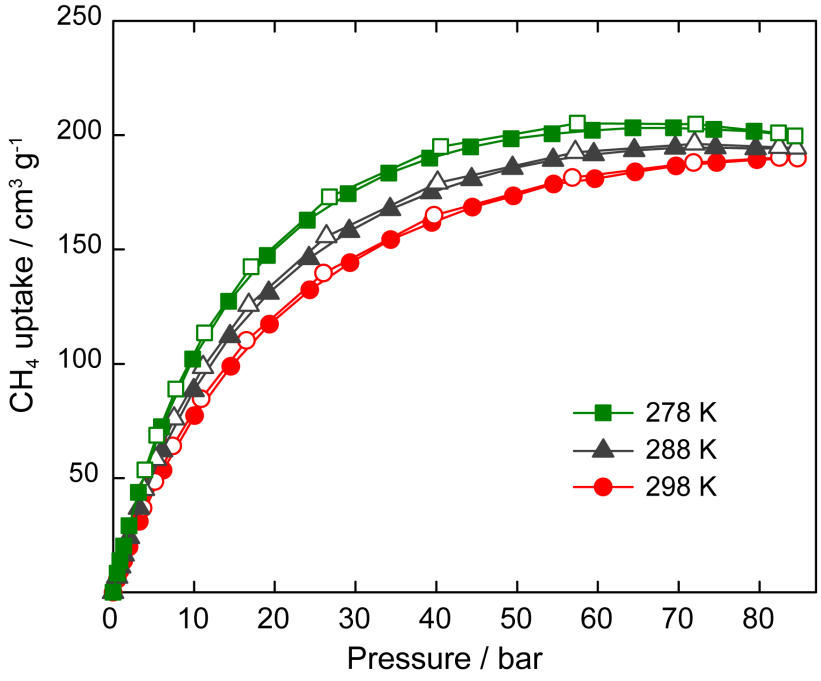


**Figure 25.** Exceed $CH_4$ adsorption isotherms for PCN-280 measured at 278, 288, and 298 K.

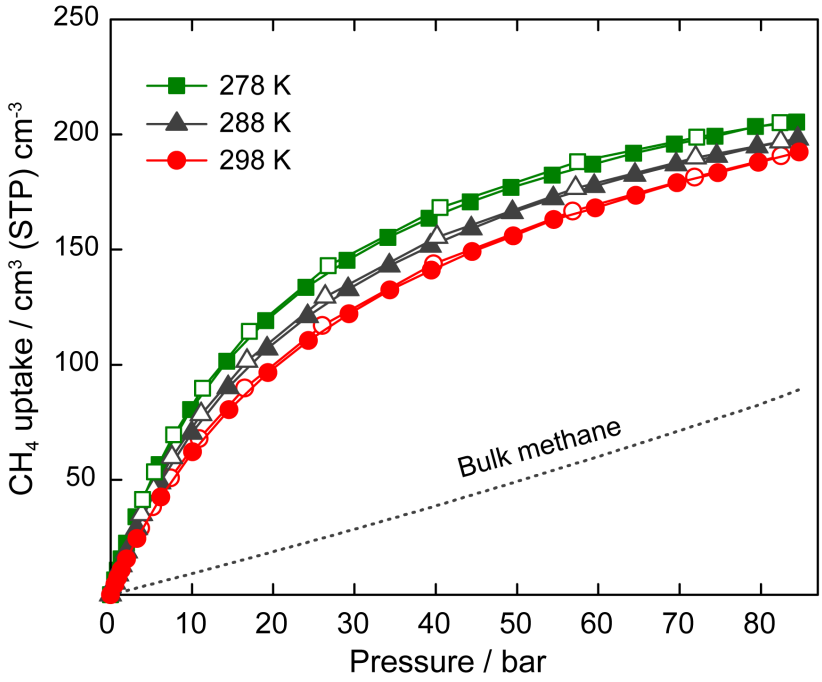


**Figure 26.** Total $CH_4$ adsorption isotherms for PCN-280 measured at 278, 288, and 298 K compared with bulk methane at room temperature.

## Section 7: References

1) H. Furukawa, N. Ko, Y. B. Go, N. Aratani, S. B. Choi, E. Choi, A. O. Yazaydin, R. Q. Snurr, M. O'Keeffe, J. Kim, O. M. Yaghi, *Science* **2010**, *239*, 424.

2) J.-F. Wang, Y.P. Wu, X.-Q. Wu, G.-X. Wen, C. Wang, *Chinese J. Struct. Chem.* **2016**, *35*, 1238.

3) D. Feng, K. Wang, Z. Wei, Y.-P. Chen, C. M. Simon, R. K. Arvapally, R. L. Martin, M. Bosch, T.-F. Liu, S. Fordham, D. Yuan, M. A. Omary, M. Haranczyk, B. Smit ang H.-C. Zhou, *Nat. Commun.* **2014**, *5*, 5723.

4) V. A. Blatov, A. P. Shevchenko, D. M. Proserpio, *Cryst. Growth Des.* **2014**, *14*, 3576.

5) M. O'Keeffe, M. A. Peskov, S. J. Ramsden, O. M. Yaghi *Acc. Chem. Res.* **2008**, *41*, 1782.